**Short title**: Mannanases necessary for glucomannan synthesis

# Atypical endo-β-1,4-mannanases are necessary for normal glucomannan synthesis in Arabidopsis

**Aina Kikuchi[1,†], Eriko Sato[1,†], Yoshihisa Yoshimi[2,3], Hironori Takasaki[1], Naho Nishigaki[1], Kimie Atsuzawa[4], Yasuko Kaneko[5], Masatoshi Yamaguchi[1], Daisuke Takahashi[1], Paul Dupree[2], and Toshihisa Kotake[1,6,*]**

**Author affiliations**:

[1]Graduate School of Science and Engineering, Saitama University, 255 Shimo-Okubo, Sakura-ku, Saitama 338-8570, Japan

[2]Department of Biochemistry, University of Cambridge, Hopkins Building, The Downing Site, Tennis Court Road, Cambridge CB2 1QW, UK

[3]Faculty of Biology-Oriented Science and Technology, Kindai University, 930 Nishimitani, Kinokawa 649-6433, Japan

[4]Comprehensive Analysis Center for Science, Saitama University, Saitama 338-8570, Japan

[5]Faculty of Education, Saitama University, 255 Shimo-Okubo, Sakura-ku, Saitama 338-8570, Japan

[6]Green Bioscience Research Center, Saitama University, 255 Shimo-Okubo, Sakura-ku, Saitama 338-8570, Japan

*Author for correspondence: kotake@mail.saitama-u.ac.jp (T. K.)

[†]These authors contributed equally to this work.

The author responsible for distribution of materials integral to the findings presented in this article in accordance with the policy described in the Instructions for Authors (https://academic.oup.com/plphys/pages/General-Instructions) is Toshihisa Kotake (kotake@mail.saitama-u.ac.jp).

**Keywords:** endo-β-1,4-mannanase, glucomannan, Golgi apparatus, membrane-anchored enzyme, quality control

**ABSTRACT**

The molecular mechanisms underlying the synthesis of large cell wall polysaccharides in plant cells are not fully understood. Here we report that two atypical endo-β-1,4-mannanases (MANs), which are not secreted and do not degrade glucomannan in the cell wall, play a novel role in glucomannan synthesis. Among the six MANs in Arabidopsis, AtMAN2 and AtMAN5 contain a transmembrane domain at their N-terminal region instead of a signal peptide. Subcellular localization using MAN protein fused with fluorescent protein demonstrated that AtMAN2 localizes to the endomembrane system including the Golgi apparatus in xylem and interfascicular fiber cells. We found that an Arabidopsis *man2 man5* double mutant lost 65% of glucomannan in the cell walls of the inflorescence stem. Immunostaining and immunoelectron microscopic observation also revealed that the *man2 man5* double mutant lost glucomannan in the cell walls to about the same extent as the *csla2 csla9* double mutant, which lacks major glucomannan synthases. A gene complementation experiment showed that the catalytic activity of AtMAN2 is important for the function in synthesis of glucomannan for the cell wall. Arabidopsis possesses another atypical MAN, AtMAN6, with an HDEL retention signal at its C-terminus. However, mutation of AtMAN6 did not affect glucomannan content in the cell walls, suggesting distinct functions for these MANs. This study has identified AtMAN2 and AtMAN5 as novel factors necessary for the normal glucomannan synthesis in Arabidopsis, along with GDP-mannose generating enzymes and CslAs, and suggests that the glucomannan hydrolysis by these MANs contributes to the maintenance of glucomannan synthesis. (249 words)

54

55 **INTRODUCTION**

56 Plant cell wall polysaccharides constitute the largest biomass carbon reservoir on earth.
57 Understanding the mechanism for their synthesis is thus indispensable for their efficient
58 production and utilization (Bar-on et al. 2018). Large polysaccharides are synthesized by
59 glycosyltransferases from building block nucleotide sugars (Verbančič et al. 2018), but
60 the molecular mechanisms are not fully understood. It is well-known that proteins
61 undergo quality control during their synthesis, which prevents protein aggregation and
62 removes unfolded proteins from the endoplasmic reticulum (ER) to be degraded in 26S
63 proteasomes in the cytosol (Mori 2000; Mayer and Bulau 2005). On the other hand, how
64 the aggregation of large cell wall polysaccharides is prevented to maintain the synthesis
65 reaction in the Golgi apparatus is still unknown.

66 Mannan polysaccharides are cell wall polysaccharides widely distributed in land plants.
67 They commonly possess a backbone composed of β-1,4-mannose (β-1,4-Man) and/or β-
68 1,4-glucose (β-1,4-Glc), while the backbone sequences and decorations are diverse
69 (Scheller and Ulvskov 2010; Voiniciuc 2022; Yoshimi et al. 2025). The backbones of
70 mannan polysaccharides can take on a two-fold structure, in which the sugar residues turn
71 at 180° resulting in a straight ribbon structure suitable for cellulose binding (Yu et al.
72 2018; 2022). Mannan polysaccharides without decoration tend to become insoluble,
73 probably as a result of intermolecular hydrogen bonding and hydrophobic interactions
74 (Chanzy et al. 1984; Zhou et al. 2018).

75 The backbones of mannan polysaccharides are synthesized from GDP-Man and GDP-

76 Glc by the action of specific glycosyltransferases, called cellulose-synthase like A (CslA)
77 proteins (Dhugga et al. 2004; Concklin et al. 1999; Liepman et al. 2005). In Arabidopsis
78 (*Arabidopsis thaliana*), CslA2 synthesizes the backbone for β-galactoglucomannan (β-
79 GGM) with alternating β-1,4-Man and β-1,4-Glc residues, whereas ClsA9 makes the
80 backbone for acetylated GGM (AcGGM) with a random sequence of β-1,4-Man and β-
81 1,4-Glc residues (Goubet et al. 2009; Yu et al. 2018; 2022, in this paper, glucomannan is
82 taken to include β-GGM and AcGGM). The reduced glucomannan content in Arabidopsis
83 *vitamin c defective1*, *konjac1*, *csla2,* and *csla9* mutants is an indication of the importance
84 of factors involved in the building block generation and the backbone synthesis reactions
85 (Conklin et al. 1999; 2000; Goubet et al. 2009; Sawake et al. 2015; Nishigaki et al. 2021).
86 These backbones subsequently undergo decoration with α-galactose by mannan α-
87 galactosyltransferase and/or acetyl groups by mannan *O*-acetyltransferase, with which the
88 solubility of glucomannan increases (Reid et al. 2003; Voiniciuc et al. 2015; Zhong et al.
89 2018; Yoshimi et al. 2025). MANNAN SYNTHESIS-RELATED (MSR) proteins are
90 other factors that have been shown to affect the glucomannan content, although their
91 molecular functions are still obscure (Wang et al. 2013). The identification of additional
92 factors is important for understanding the molecular mechanism of glucomannan
93 synthesis.
94 Endo-β-1,4-mannanase (MAN) is one of the conserved cell wall enzymes in plants,
95 belonging to the glycoside hydrolase (GH) 5 family (Aspeborg et al. 2021). The
96 physiological importance of MANs has been extensively studied in seed germination and
97 fruit ripening (Nonogaki et al. 2000; Schröder et al. 2004; Belotserkovsky et al. 2007;

98 Iglesias-Fernández et al. 2011). Based on domains, motifs, and sequence similarity, plant
99 MANs can be classified into several types (Fig. 1A) (Wang et al. 2014). Arabidopsis
100 secreted type MANs, AtMAN3 and AtMAN7, hydrolyze cell wall glucomannan to
101 contribute to cadmium tolerance via activation of phytochelatin and glutathione synthesis
102 (Chen et al. 2015; Wu et al. 2023). AtMAN6 is a HDEL-type MAN with a C-terminal
103 HDEL signal, which is a retrograde transport signal back from the Golgi apparatus to the
104 ER (Alvim et al. 2023). AtMAN6 and its poplar (*Populus trichocarpa*) orthologue,
105 PtrMAN6, are specifically localized in vessel cells and presumed to release GGM
106 oligosaccharides as signaling molecules, which negatively regulate secondary cell wall
107 formation in the vessel and interfascicular fiber cells (Zhao et al. 2013; Zhang et al. 2023).
108 On the other hand, AtMAN2 and AtMAN5 are a different type of MAN with a
109 transmembrane (TM) domain instead of a signal peptide in the N-terminal region,
110 designated TM-type MANs here. Recombinant AtMAN2 expressed in *Escherichia coli*
111 shows hydrolytic activity toward mannan polysaccharides and lacks transglycosylation
112 activity (Wang et al. 2015), but its physiological importance and functions remain to be
113 studied.
114 This study focused on the importance and functions of the TM-type MANs, AtMAN2
115 and AtMAN5, comparing them with another atypical MAN, AtMAN6, in glucomannan
116 synthesis. The analysis of Arabidopsis loss-of-function mutants suggested that the
117 hydrolysis of glucomannan by AtMAN2 and AtMAN5 is necessary for normal
118 glucomannan synthesis, where their roles must thus be different from that of AtMAN6.
119 These findings provide new insights into the synthesis of plant cell wall polysaccharides.

120

121 **RESULTS**

122 **TM-type MANs are conserved in angiosperms**

123 In Arabidopsis, two TM-type MANs, AtMAN2 (AT2G20680) and AtMAN5
124 (AT4G28320), are highly related in their amino acid sequences (identity, 83%), while
125 AtMAN6 (AT5G01930) is the sole HDEL-type MAN (Fig. 1A). TM-type MANs can be
126 found in other angiosperms including amborella (*Amborella trichopoda*) and rice (*Oryza*
127 *sativa*), forming a clade apart from the secreted type MANs in the phylogenetic tree (Fig.
128 1B). On the other hand, *Physcomitrium patens* (a moss species) and *Marchantia*
129 *polymorpha* (a liverwort species) lack this type. The HDEL-type MANs also formed a
130 different clade, which did not include MANs from *P. patens* and *M. polymorpha*. The
131 distribution and phylogenetic relationships suggest that the TM-type MANs have
132 functions different from the secreted and the HDEL-type MANs.

133

134 **Loss of glucomannan in *man2 man5* double mutants**

135 Because high sequence similarity suggested functional redundancy of AtMAN2 and
136 AtMAN5, an Arabidopsis *man2-1 man5-1* double mutant was generated for functional
137 analysis. The double mutants did not show significant growth defects in the seedlings
138 (Supplementary Fig. S1). In addition, although the double mutants had slightly shorter
139 inflorescence stems than wild type (WT) plants as was also observed for the *csla2-2*
140 *csla9-2* double mutants, they did not show severe growth defects (Yu et al. 2022)
141 (Supplementary Fig. S2). Based on the expression patterns (Winter et al. 2007), *AtMAN2*

142 and *AtMAN5* are presumed to function in the inflorescence stem (Supplementary Fig. S3).

143 To examine the importance of AtMAN2 and AtMAN5 for glucomannan accumulation,
144 we observed the cross sections of the bottom part of inflorescence stems of Arabidopsis
145 *man2-1* single, *man2-2* single, *man5-1* single, and *man2-1 man5-1* double mutants and
146 compared them with WT with LM21 antibody specific to glucomannan (Thorne et al.
147 2023). Although MANs are hydrolytic enzymes acting on mannan polysaccharides (Wang
148 et al. 2015), the glucomannan signals were, unexpectedly, almost lost in the cell walls of
149 the *man2-1 man5-1* double mutant as they were in the *csla2-2 csla9-2* double mutant,
150 while the signals were observed in the single mutants as they were in the WT, indicating
151 the functional redundancy of AtMAN2 and AtMAN5 (Fig. 2). To examine the functional
152 relationships of AtMAN2 and AtMAN5 with AtMAN6, the cross sections of the *man6-1*
153 single, the *man2-1 man6-1* double, the *man5-1 man6-1* double, the *man2-1 man5-1 man6-*
154 *1* triple, and the *man2-2 man5-1 man6-1* triple mutants were also observed. The cell wall
155 glucomannan signals were almost lost in the triple mutants as in the *man2-1 man5-1*
156 double mutant but remained in the other double mutants (Fig. 2), suggesting that the
157 AtMAN2 and AtMAN5 contribution to the glucomannan accumulation differs from that
158 of AtMAN6. Xylan, together with cellulose, is a major component of secondary cell walls,
159 but immunostaining with LM10 antibody specific to xylan did not point to compensatory
160 changes in the mutants (Supplementary Fig. S4). The TM-type MANs do not seem to
161 influence the content of other cell wall polysaccharides in the inflorescence stem.

162

163 **Drastic decrease of cell wall glucomannan in the double and triple mutants**

164 The changes in the glucomannan accumulation in the inflorescence stems of the *man2-1*
165 *man5-1* double and the *man2-1 man5-1 man6-1* and the *man2-2 man5-1 man6-1* triple
166 mutants were further investigated by cell wall fractionation and subsequent sugar
167 composition analysis. The cell walls were fractionated into water-soluble fraction (soluble
168 fraction), alkali-extractable fraction (alkali fraction), and cellulose fraction (Fig. 3A;
169 Supplementary Fig. S5), and the sugar composition of these fractions was determined by
170 high-performance anion-exchange chromatography with pulsed amperometric detection
171 (HPAEC-PAD) (Supplementary Fig. S6). Consistent with the immunostaining of
172 glucomannan with LM21 in the cross sections (Fig. 2), the *man2-1 man5-1* double and
173 the *man2-1 man5-1 man6-1* and *man2-2 man5-1 man6-1* triple mutants lost more than
174 65% mannose in these cell wall fractions (Fig. 3B). As other hemicelluloses and pectin
175 rarely have mannose residues in Arabidopsis (Mohnen 2008; Goubet et al. 2009; Scheller
176 and Ulvskov 2010), this result indicates that the double and triple mutants lost a large part
177 of its glucomannan. It has been reported that AtMAN6 negatively regulates secondary
178 cell wall thickening (Zhang et al. 2023), but neither mannose content nor the sugar content
179 proportion of cell wall fractions was changed in the *man6-1* mutant (Fig. 3).
180 The Arabidopsis inflorescence stem has two different glucomannans, β-GGM and
181 AcGGM, which are synthesized by CslA2 and CslA9, respectively (Goubet et al. 2009;
182 Yu et al. 2018; 2022). The influence of the loss of TM-type MANs on these glucomannans
183 was evaluated by polysaccharide analysis using carbohydrate gel electrophoresis (PACE)
184 (Supplementary Fig. S7). Here, β-GGM and AcGGM included in the stem cell walls were
185 hydrolyzed into oligosaccharides by a microbial MAN, CjMan26A, separated, and

186 detected (Hogg et al. 2001). The *man2-1 man5-1* double and the triple mutants with
187 *man6-1* showed almost no β-Glc-(β-Gal-α-Gal-)β-Man-β-Glc-(α-Gal-)β-Man-β-Glc-
188 Man (GBGAGM) and β-Glc-(β-Gal-α-Gal-)β-Man-β-Glc-Man (GBGM)
189 oligosaccharides from β-GGM and no β-Glc-β-Glc-Man (GGM) and β-Glc-β-Man-Man
190 (GMM) from AcGGM (Supplementary Fig. S7), so they were similar to the *csla2-2 csla9-*
191 *2* double mutant in this respect (Goubet et al. 2009) (Fig. 4). These results demonstrate
192 that the TM-type MANs are necessary for the normal synthesis of both β-GGM and
193 AcGGM in the inflorescence stem.
194
195 **Retention of glucomannan in the vacuole**
196 β-GGM and AcGGM are synthesized in the Golgi apparatus by CslA2 and CslA9,
197 respectively, then secreted to the cell walls. While the expression levels of these *CslA*
198 genes did not decrease (Supplementary Fig. S8), the glucomannan amount drastically
199 decreased (Figs. 3 and 4). To gain insight into the functions of AtMAN2 and AtMAN5,
200 the glucomannan in the cross sections of *man* mutants was observed at high magnification.
201 Although the *man2-1 man5-1* double and the *man2-1 man5-1 man6-1* triple mutants lost
202 most cell wall glucomannan as shown in Fig. 3, these mutants contained relatively large
203 (>1 μm) particles detected with LM21 antibody inside the xylem and interfascicular fiber
204 cells of the bottom part of inflorescence stems (Fig. 5A). Importantly, glucomannans
205 inside cells have also been observed in Arabidopsis and other plants such as aloe (*Aloe*
206 *vera*) (Ahl et al. 2019; Handford et al. 2003; Herburger et al. 2022), although these
207 glucomannans have not been identified. Because the particles significantly decreased in

208 the *csla2-2 csla9-2* double mutant, most of these particles can be presumed to be β-GGM
209 and AcGGM that were not secreted to the cell walls. On the other hand, the particles that
210 remained even in the *csla2-2 csla9-2* double mutant may be glucomannan synthesized by
211 different CslAs from CslA2 and Csla9. Although significant differences from WT were
212 not observed, these particles tended to increase rather than decrease in the double and
213 triple mutants (Fig. 5B).

214 To identify the glucomannan particles retained inside cells, immunoelectron
215 microscopy was conducted. In this experiment, the glucomannans in the ultrathin cross
216 sections from the bottom part of inflorescence stems of the *man2-1 man5-1* double and
217 the *man2-1 man5-1 man6-1* triple mutants were recognized by LM21 as the primary
218 antibody and visualized with a secondary antibody conjugated to gold particles.
219 Consistent with immunostaining and cell wall analysis, there were fewer gold particles in
220 the cell walls of the triple mutant, showing loss of glucomannan in the cell walls.
221 Relatively large clusters (>1 μm) of gold particles were found in the vacuole in the triple
222 mutant (Fig. 5C). These observations suggest that the glucomannan particles are formed
223 and retained in the vacuole in the absence of the TM-type MANs, AtMAN2 and AtMAN5.
224

225 **Tissue and subcellular localization of AtMAN2 and AtMAN6 differ**

226 The tissue and subcellular localization of AtMAN2 and AtMAN5 was investigated using
227 transgenic Arabidopsis harboring *pMAN2::MAN2TM-mNeon* or *pMAN5::MAN5TM-*
228 *mNeon* in which the fluorescent protein mNeonGreen sequence was inserted right behind
229 the TM domain in the genomic sequences (Supplementary Fig. S9). In this experiment,

230 the gene constructs were introduced into the *man2-1 man5-1 man6-1* or the *man2-2 man5-*
231 *1 man6-1* triple mutants. Immunostaining of the cross sections of the bottom part of
232 inflorescence stems showed that AtMAN2TM-mNeon and AtMAN5TM-mNeon at least
233 partially restored impaired glucomannan accumulation in the triple mutants
234 (Supplementary Fig. S9). For microscopic observation, the top part of the inflorescence
235 stem was chosen because strong mNeonGreen signals were found there. The
236 AtMAN2TM-mNeon signal was widely observed in the xylem and interfascicular fiber
237 cells of inflorescence stems (Supplementary Fig. S10). The AtMAN2TM-mNeon signal
238 was not found in the cell walls but localized in the compartments (Fig. 6A-E), suggesting
239 that AtMAN2 functions in the endomembrane including the Golgi apparatus. The
240 AtMAN5TM-mNeon signal was also found inside cells (Fig. 6F-J), although the
241 localization was not clear because of low signal intensity.

242 To compare, we also generated *pMAN6::MAN6signal-mNeon* in which the
243 mNeonGreen sequence was inserted after the signal peptide into the genomic *AtMAN6*
244 sequence (Supplementary Fig. S9). Contrasting with AtMAN2TM-mNeon signals, the
245 AtMAN6signal fluorescence was limited to developing vessels (Supplementary Fig. S10).
246 The fluorescence was spread in the vessel cells (Fig. 6K-O), indicating its localization in
247 the ER or the vacuole. Previously it was suggested that AtMAN6 localizes on the plasma
248 membrane (PM), but this was using a C-terminal fusion of AtMAN6 with green
249 fluorescent protein, which might have affected the localization. But in that study, as in
250 this, AtMAN2 and AtMAN6 were found in substantially different locations, indicating
251 that they have different molecular functions (Zhang et al. 2023).

252

253 **The catalytic activity of AtMAN2 and AtMAN5 is required**

254 To determine the importance of the catalytic activity of AtMAN2, we performed a gene
255 complementation experiment on the *man2-1 man5-1* double mutant using point-mutated
256 genomic *AtMAN2* gene in which the catalytic residues were replaced with Ala (E215A
257 and E335A in AtMAN2). The mutated *AtMAN2* gene failed to restore the glucomannan
258 accumulation detected with the LM21 antibody in the inflorescence stem of the double
259 mutant (Supplementary Figs. S9, S11). This result suggests that for proper functioning of
260 the glucomannan synthesis in the Golgi apparatus, the catalytic activity of AtMAN2 is
261 necessary.

262

263 **DISCUSSION**

264 **MANs are newly recognized as necessary for normal glucomannan synthesis**

265 The present study has identified AtMAN2 and AtMAN5 as factors necessary for normal
266 glucomannan synthesis in Arabidopsis, to work along with VTC1 and KJC1 generating
267 GDP-Man, CslAs catalyzing the glucomannan backbone synthesis, and MSRs (Conklin
268 et al. 1999; Goubet et al. 2009; Wang et al. 2013; Yu et al. 2014; Sawake et al. 2015;
269 Nishigaki et al. 2021). Based on the distribution of orthologues, it is likely that many
270 angiosperms utilize TM-type MANs in glucomannan synthesis.

271 Because the expression levels of *CslA2* and *CslA9* did not decrease in the *man2-1*
272 *man5-1* double and the *man2-1 man5-1 man6-1* triple mutants (Supplementary Fig. S8),
273 we infer that the decreased glucomannan in the mutants was not caused by changes in the

274 expression of *CslA* genes and that AtMAN2 and AtMAN5 contribute to glucomannan
275 synthesis through their enzymatic activity. The requirement of polysaccharide degrading
276 enzymes for polysaccharide synthesis presents an apparent paradox. Yet this is not the
277 first example: among other plant glycoside hydrolases, the membrane-associated GH9
278 endo-β-1,4-glucanase KORRIGAN1 (KOR1) is well known for its role in cellulose
279 synthesis (Nicol et al. 1996). The Arabidopsis *kor1* mutant suffers severe defects in the
280 synthesis of cellulose, demonstrating the importance of this protein. The sea squirt *Ciona*
281 *intestinalis* and bacteria such as *Agrobacterium tumefaciens* and *Acetobacter xylinum* also
282 require endo-β-1,4-glucanases for their cellulose synthesis. These enzymes belong to the
283 GH6 and 8 families and are thus distinct from KOR1 (Standal et al. 1994; Matthysse et
284 al. 1995; Li et al. 2023). These observations imply that hydrolytic activity of endo-β-1,4-
285 glucanases is important to facilitate cellulose synthesis. The present study describes a
286 second instance of a version of this paradox in polysaccharide synthesis. We suggest that
287 this paradox may represent a general mechanism to prevent the aggregation of newly
288 synthesized cell wall polysaccharides in plant cells.
289
290 **Not all CslAs require TM-type MANs for glucomannan synthesis**
291 The TM-type MANs are not necessarily required for all glucomannan synthesis by CslAs
292 in plants. In the present study, the alkali fraction from the inflorescence stems of *man2-1*
293 *man5-1* double mutant still contained 30% of mannose compared with WT (Fig. 3B).
294 Because *N*-glycosylated proteins with mannose residues would not have been collected
295 in the alkali fraction, there seems to be mannan polysaccharide synthesized independently

296 from the functions of AtMAN2 and AtMAN5. This unknown mannan polysaccharide
297 would have to be resistant to hydrolysis by CjMan26A used for PACE.
298 Many green algae and bryophytes such as *P. patens* and *M. polymorpha* have mannan
299 polysaccharides as major cell wall components (Kolkas et al. 2023; Chernova et al. 2024),
300 although they lack genes orthologous to *AtMAN2* and *AtMAN5* (Fig, 1B). To understand
301 the molecular mechanism for the glucomannan synthesis involving TM-type MAN,
302 future research should try to clarify which types of mannan polysaccharides require these
303 MANs.
304
305 **Putative function of AtMAN2 and AtMAN5 in quality control**
306 AtMAN2TM-mNeon localized in the endomembrane including the Golgi apparatus in
307 the inflorescence stem (Fig. 6). In the gene complementation experiment, the genomic
308 *AtMAN2* gene with mutations at catalytic residues failed to restore cell wall glucomannan
309 in the *man2 man5* double mutant (Supplementary Fig. S11). Recently, AtMAN2 and
310 AtMAN5 were also shown to increase soluble mannan polysaccharides in Pichia yeast
311 (*Pichia pastoris*) expressing Arabidopsis *CslA2* (Jacobson et al. 2025). It has been
312 reported that AtMAN2 lacks transglycosylation activity (Wang et al. 2015). Based on
313 these facts, we suggest that glucomannan undergoes hydrolysis by AtMAN2 and
314 AtMAN5 after the synthesis in the Golgi apparatus. The drastic decrease in the
315 glucomannan content in the double and triple mutants implies that the continuous
316 synthesis reaction by CslAs is not maintained in these mutants. The alternative, that only
317 secretion is impaired in the mutants, while the glucomannan synthesis by CslA2 and

318 CslA9 is maintained, does not seem likely, because in this case the glucomannan would
319 have been collected in one of the fractions (Fig. 3B). We cannot specify the molecular
320 functions of these MANs in detail, but it is conceivable that large β-GGM and AcGGM
321 molecules synthesized by CslA2 and CslA9 before decoration easily aggregate during
322 synthesis, which may cause the termination of the chain elongation reaction by these
323 CslAs. This problem may be alleviated through removal by partial hydrolysis with these
324 MANs as polysaccharides generally become more soluble through hydrolysis into shorter
325 chains. These reactions to prevent aggregate formation and to remove aggregates in the
326 Golgi apparatus can be considered analogous to the protein quality control in the ER
327 (Mori 2000; Oda et al. 2003). It is also probable that AtMAN2 and AtMAN5 facilitate the
328 release of glucomannan from CslA proteins by partial hydrolysis during synthesis,
329 enabling its proper loading into the secretion pathway. The impairment of this process
330 may also negatively affect glucomannan synthesis by CslAs.
331 In xyloglucan, the importance of galactose-side chains to avoid aggregation has been
332 shown (Tamura et al. 2005; Kong et al. 2015; Hoffmann and McFarlane 2024). The
333 Arabidopsis *murus3* mutant, which lacks galactose-side chains on its xyloglucan, suffers
334 intracellular aggregation of xyloglucan in the roots, resulting in growth defects. It is
335 probable that such intracellular aggregation was avoided through the termination of the
336 synthesis reaction in the *man2-1 man5-1* double mutant. Clarifying this mechanism will
337 presumably require the identification of as yet unknown factors involved in this reaction.
338

339 # MATERIALS AND METHODS

340 **Arabidopsis mutants and growth conditions**

341 *Arabidopsis thaliana* ecotype Col-0 was used in this study. The T-DNA insertion lines
342 SALK_0383344 (*man2-1*), SALK_016450 (*man2-2*), SALK_059047 (*man5-1*), and
343 SALK_129977 (*man6-1*) were provided by the Arabidopsis Biological Resource Center.
344 The double and triple mutants were generated by crosses between these mutants. The
345 genotypes of the mutants were determined using specific primers (Supplementary Fig.
346 S12 and Table S1). The *csla2-2 csla9-2* and *msr1-1 msr2-2* double mutants had been
347 obtained in our previous studies (Goubet et al. 2007; 2009; Wang et al. 2013). Arabidopsis
348 seeds were sterilized and sown on Murashige and Skoog (MS) medium in 0.8% (w/v)
349 agar. After stratification at 4 °C in the dark for 2 days, the seeds were germinated and
350 grown under continuous light (cold cathode fluorescent lamp; Biomedical Science) at
351 23 °C for 10 days, then on rockwool fiber for 4 weeks under continuous light at 23 °C.

352 For the gene complementation experiment, a genomic DNA fragment for *AtMAN2* was
353 amplified by PCR and subcloned into the binary vector pBGGN (Inplanta Innovation,
354 Yokohama, Japan). The point mutations at the catalytic sites were introduced by PCR
355 with specific primers (Supplementary Table S1). The *man2-1 man5-1* double mutant was
356 transformed with mutated AtMAN2/pBGGN and WT AtMAN2/pBGGN by an
357 Agrobacterium-mediated (*Rhizobium radiobacter*, EHA105 strain) method (Clough and
358 Bent 1998).

359

360 **Phylogenetic analysis**

361 The amino acid sequences of MANs from various plants were collected using Basic Local
362 Alignment Search Tool in NCBI (https://blast.ncbi.nlm.nih.gov/Blast.cgi)
363 (Supplementary Table S2). The signal peptide and TM region were detected using the
364 SignalP 6.0 and TMHMM-2.0 programs, respectively (Teufel et al. 2022; Krogh et al.
365 2001; Moller et al. 2001). The alignments of amino acid sequences were performed by
366 the MUSCLE program in MEGA software (version 11; Tamura et al. 2021) with default
367 parameters. The phylogenetic trees were generated using the maximum likelihood method
368 with 100 bootstraps.
369
370 **Cell wall fractionation and sugar composition analysis**
371 The bottom part of first inflorescence stem 2 weeks after bolting (approximately 50 mg)
372 was homogenized with mortar and pestle in water (Supplementary Fig. S4). After
373 centrifugation at 10,000 x g at 4°C for 5 min, the supernatant was collected as the soluble
374 fraction. The precipitate was suspended in 0.4 mL of 4 M potassium hydroxide (KOH)
375 containing 0.04% (w/v) sodium borohydride at 25°C. After centrifugation at 10,000 x g
376 at 4°C for 5 min, the supernatant was collected. This extraction was repeated. The
377 combined supernatant (0.8 mL) was neutralized with 0.4 mL of glacial acetic acid and
378 collected as the alkali fraction. The precipitate was washed with 98% (v/v) ethanol, 2%
379 (v/v) acetic acid twice, lyophilized for 24 h, hydrolyzed with 72% (v/v) sulfuric acid at
380 4 °C for 1 h and 8% (v/v) sulfuric acid at 100 °C for 4 h, and then collected as the cellulose
381 fraction. Total sugar composition and quantity of the above fractions were determined
382 using the phenol sulfuric acid procedure (Dubois et al. 1956).

383 For sugar composition analysis, the alkali fraction was dialyzed against water at 4 °C
384 for 2 days. The soluble and alkali fractions were hydrolyzed into monosaccharides with
385 2 M trifluoroacetic acid (TFA) at 121 °C for 1 h, then lyophilized to remove TFA. The
386 cellulose fraction after the hydrolysis with sulfuric acid was neutralized with barium
387 carbonate and desalted with Dowex beads (Dowex 50WX8, Dow Chemical).
388 Monosaccharide composition was determined by HPAEC-PAD using a Dionex ICS-
389 5000+ liquid chromatograph (Thermo Fisher Scientific) fitted with a CarboPac PA-1
390 column (Thermo Fisher Scientific) and a pulsed amperometric detector (Thermo Fisher
391 Scientific) as described previously (Sawake et al. 2015).
392
393 **PACE**
394 Alcohol-insoluble residue (AIR) was prepared from the bottom part of Arabidopsis
395 inflorescence stems (fresh weight, 100 mg) according to Yu et al. (2018). Glucomannans
396 were extracted from the AIR with 1 mL of 4 M potassium hydroxide solution by shaking
397 at 1,000 rpm at room temperature for an hour. After centrifugation at 15,000 x g for 15
398 minutes, the supernatant was collected. To collect remaining glucomannans, the pellet
399 was suspended in 1 mL of water. After centrifugation, the supernatant was collected. The
400 supernatants were combined and applied to a PD-10 column (Cytiva) to exchange the
401 solvent with 50 mM ammonium acetate buffer (pH 6.0). The eluted fraction was used as
402 the KOH fraction.
403 Glucomannans in the KOH fraction were hydrolyzed into specific oligosaccharides

404 with a commercial endo-β-1,4-mannanase, CjMan26A (1 unit, E-BMACJ, Megazyme),
405 from *Cellvibrio japonicus* in 50 mM ammonium acetate buffer (pH 6.0) at 37 °C
406 overnight (Supplementary Fig. S7) (Hogg et al. 2001). After the reaction, the enzyme was
407 denatured by heating at 100 °C for 15 minutes. The oligosaccharides were derivatized
408 with 8-aminonapthalene-1,3,6-trisulphonic acid, resuspended in urea, and separated by
409 electrophoresis as described (Goubet et al. 2009; Yoshimi et al. 2025). Gels were
410 visualized using a G-Box (Syngene, Cambridge, UK) with a transilluminator with long-
411 wave tubes emitting at 365 nm and a shortpass (500 to 600 nm) detection filter. Mannose
412 and β-1,4-mannooligosaccharides ($Man_{2-6}$, Megazyme) were used as standards.
413

414 **Immunostaining of glucomannan in the mutants**

415 The glucomannan and xylan in the inflorescence stems were observed using specific
416 antibodies. The bottom part of inflorescence stems (the lowest one-sixth portion) was
417 fixed with 4% (v/v) paraformaldehyde and 0.6% (v/v) glutaraldehyde at 4 °C for 3 h. The
418 fixed samples were dehydrated through a graded ethanol series, embedded in Technovit
419 7100 (Nisshin EM, Tokyo, Japan) using a graded series of ethanol and Technovit 7100
420 mixtures, and solidified with Technovit hardener (Nisshin EM) at 60 °C for 12 h. Sections
421 were sliced to a thickness of 10 μm using a microtome (RM2125RT; Leica, Tokyo, Japan)
422 equipped with a disposable steel blade (C35; Feather, Osaka, Japan).

423 To remove acetyl groups from polysaccharides, the cross-sections were treated with 50
424 mM sodium hydroxide at 25 °C for 30 min. The sections were then washed with
425 phosphate-buffered saline (PBS) containing 137 mM NaCl, 10 mM disodium

426 hydrogenphosphate, 2.7 mM KCl, and 1.8 mM potassium dihydrogenphosphate (pH 7.4)
427 and then blocked in PBS containing 0.3% (w/v) blocking milk (Sigma-Aldrich, Tokyo,
428 Japan) for 30 min. Then, the sections were incubated for 1.5 h with antibodies against
429 glucomannan (LM21, Kerafast, Shirley, MA; dilution 1:5) or xylan (LM10, Kerafast;
430 dilution 1:5) in PBS with blocking milk. After washing three times with PBS, the sections
431 were incubated for 1 h with Alexa Fluor 488-conjugated anti-mouse IgM for LM21
432 (abcam, Cambridge, UK; dilution 1:100) or Alexa Fluor 488-conjugated anti-mouse IgG
433 for LM10 (abcam; dilution 1:100) in PBS with bovine serum albumin (Thorne et al. 2023).
434 The sections were washed three additional times with PBS. The cross sections were
435 imaged with a microscope (ECLIPSE Ci-L Plus, Nikon, Japan) at 488 nm. The dark field
436 image was also acquired simultaneously.
437
438 **Immunoelectron microscopy**
439 Immunoelectron microscopy to detect the glucomannan localization was performed
440 according to Atsuzawa et al. (2010). The bottom part (the lowest one-sixth portion) and
441 upper part (the highest one-sixth portion) of the inflorescence stems of WT, the *man6-1*
442 single, the *man2-1 man5-1* double, and the *man2-1 man5-1 man6-1* triple mutants were
443 fixed with 2% (v/v) glutaraldehyde in 50 mM potassium phosphate (pH 6.8) at room
444 temperature for 3 h. After washing with 100 mM lysine in 50 mM potassium phosphate
445 (pH 6.8) the samples were dehydrated in a graded ethanol series. The tissues were
446 embedded in LR White resin (Electron Microscopy Sciences, USA) and polymerized by

447 heating at 60 °C. Ultrathin sections of 100 nm thickness were cut on an UltracutN
448 ultramicrotome (Nissei) and collected on nickel grids coated with polyvinyl formvar
449 membrane.

450 Ultra-thin sections were immersed in 50 mM sodium hydroxide at room temperature
451 for 30 min and washed with Tris-HCl buffer (TBS: 50 mM Tris-HCl (pH 7.5), 150 mM
452 sodium chloride) containing 0.05% Triton X-100 (TBS/Tx). They were treated with
453 blocking solution (10 mg/ml bovine serum albumin in TBS) at room temperature for 60
454 min, and they were incubated with LM21 antibody at 1:500 dilution at 4 °C overnight.
455 After washing with TBS/Tx, the sections were incubated with a solution of 10 nm gold
456 particles conjugated with goat anti-rat IgG (BBI solutions, UK) as the secondary antibody
457 at a 1:30 dilution for 1 h at room temperature and washed with TBS/Tx. Specimens were
458 observed with a transmission electron microscope (H-7500, Hitachi, Japan) at an
459 accelerating voltage of 80 kV after staining with uranyl acetate and lead citrate.
460

461 **Transgenic plants expressing MAN-mNeonGreen**

462 For the generation of transgenic Arabidopsis harboring *pMAN2::MAN2TM-mNeon*,
463 *pMAN5::MAN5TM-mNeon*, or *pMAN6::MAN6signal-mNeon*, the DNA fragments of
464 genomic *AtMAN2*, *AtMAN5*, and *AtMAN6* and mNeonGreen were amplified from
465 Arabidopsis genomic DNA and template mNeonGreen (Addgene, #189976), respectively,
466 using the primer sets listed in Supplementary Table S1. The DNA fragments were
467 assembled and subcloned into the binary vector pBGGN with DNA assembly kit (Gibson)
468 to yield the constructs, *pMAN2::MAN2TM-mNeon/pBGGN*, *pMAN5::MAN5TM-*

469 *mNeon/pBGGN* and *pMAN6::MAN6signal-mNeon/pBGGN* (Supplementary Fig. S9).
470 These constructs were introduced into the *man2-1 man5-1 man6-1* or the *man2-2 man5-*
471 *1 man6-1* triple mutants by an Agrobacterium-mediated (*Rhizobium radiobacter*,
472 EHA105 strain) method (Clough and Bent 1998).
473
474 **Observation of tissue and subcellular localization of MAN-mNeonGreen proteins**
475 Cross sections were excised from the top part of the inflorescence stems of
476 *pMAN2::MAN2signal-mNeon* (line #3), *pMAN2::MAN2signal-mNeon* (line #4), and
477 *pMAN6::MAN2signal-mNeon* (line #3) plants and stained with 6.34 μM fixable analog of
478 N-(3-triethylammoniumpropyl)-4-(6-(4-(diethylamino) phenyl) hexatrienyl) pyridinium
479 dibromide, FM 4-64FX (ThermoFisher). The confocal images were obtained using a
480 Zeiss LSM800 (Zeiss, Jena, Germany) with a Plan-Apochromat 63×/1.4 oil immersion
481 objective lens. FM 4-64FX was excited at 561 nm and detected between 400 and 645 nm.
482 Fluorescence signals from mNeonGreen were detected after excitation at 488 nm and
483 detected at 410-546 nm. Autofluorescence was excited at 488 nm and detected at 550-700
484 nm. Transmitted photomultiplier tube (T-PMT) images were also captured during
485 confocal imaging.
486
487 **Author Contributions**: T.K. and P.D. designed the research. A.K., E.S., Y.Y., H.T., N.N.,
488 K.A., Y.K., D.T., and T.K. performed research. E.S., Y.Y., D.T., Y.K., and T.K. analyzed
489 the data. H.T., Y.K., D.T., P.D., and T.K. wrote the manuscript.

**Conflict of interest**

The authors declare no conflict of interest.

**Acknowledgments**: We thank Dr. Kiminori Toyooka from RIKEN and Prof. Masatsugu Toyota and Dr. Hiraku Suda from Saitama University for valuable discussions. This work was supported by MEXT KAKENHI Grant-in-Aid for Scientific Research to T. Kotake [no. 18H05495], Grant-in-Aid for Scientific Research to T. Kotake [no. 23H04302 and no. 23H02134] and to D. Takahashi [no. 23K05144 and no. 24KK0273], the ERC Advanced Grant EVOCATE to P. Dupree funded by the United Kingdom Research and Innovation (UKRI) grant number EP/X027120/1 (www.ukri.org) and by the grant OpenPlant (UKRI BBSRC, BB/L014130/1) to P. Dupree, and a Broodbank Research Fellowship to Y. Yoshimi (reference no. PD16178).

## Supplementary Data

**Supplementary Table S1.** Primers used for genotyping, plasmid construction, and point mutations.

**Supplementary Table S2.** List of MAN sequences in the phylogenetic analysis.

**Supplementary Fig. S1.** Growth phenotypes of seedlings of *man* mutants

**Supplementary Fig. S2.** Growth phenotypes in the inflorescence stems of *man* mutants

**Supplementary Fig. S3.** Expression patterns of *AtMAN2*, *AtMAN5*, and *AtMAN6* genes.

511 **Supplementary Fig. S4.** Xylan accumulation in *man* mutants.

512 **Supplementary Fig. S5** Cell wall fractionation from inflorescence stems.

513 **Supplementary Fig. S6.** Monosaccharide composition of the soluble, alkali, and

514 cellulose fractions.

515 **Supplementary Fig. S7.** Oligosaccharides detected by PACE.

516 **Supplementary Fig. S8.** Expression levels of *CslA2* and *CslA9* in *man* mutants.

517 **Supplementary Fig. S9.** Gene constructs and complementation of *man* mutants.

518 **Supplementary Fig. S10.** Tissue localization of MAN-mNeon proteins.

519 **Supplementary Fig. S11.** Gene complementation experiment with mutated genomic

520 *AtMAN2* and *AtMAN5* genes.

521 **Supplementary Fig. S12.** T-DNA insertion sites and genotyping of *man* mutants.

522

523

## LITERATURE CITED


**Ahl LI, Mravec J, Jørgensen B, Rudall PJ, Rønsted N, Grace OM.** Dynamics of intracellular mannan and cell wall folding in the drought responses of succulent Aloe species. *Plant Cell Environ*. 2019:42(8):2458-2471. https://doi.org/10.1111/pce.13560

**Alvim JC, Bolt RM, An J, Kamisugi Y, Cuming A, Silva-Alvim FAL, Concha JO, daSilva LLP, Hu M, Hirsz D, Denecke J.** The K/HDEL receptor does not recycle but instead acts as a Golgi-gatekeeper. *Nat Commun.* 2023:14(1):1612. https://doi.org/10.1038/s41467-023-37056-0

**Aspeborg H, Coutinho PM, Wang Y, Brumer H 3rd, Henrissat B.** Evolution, substrate specificity and subfamily classification of glycoside hydrolase family 5 (GH5). *BMC Evol Biol.* 2012:12:186. https://doi.org/10.1186/1471-2148-12-186

**Atsuzawa K, Nakazawa A, Mizutani K, Fukasawa M, Yamamoto N, Hashimoto T, Usuda N.** Immunohistochemical localization of mitochondrial fatty acid β-oxidation enzymes in Müller cells of the retina. *Histochem Cell Biol*. 2010:134(6):565-579. https://doi.org/10.1007/s00418-010-0752-4

**Bar-On YM, Phillips R, Milo R.** The biomass distribution on Earth. *Proc Natl Acad Sci USA.* 2018:115(25):6506-6511. https://doi.org/10.1073/pnas.1711842115

**Belotserkovsky H, Berger Y, Shahar R, Wolf S**. Specific role of LeMAN2 in the control of seed germination exposed by overexpression of the LeMAN3 gene in tomato plants. *Planta.* 2007:227(1):199-209. https://doi.org/10.1007/s00425-007-0607-y

**Chanzy HD, Grosrenaud A, Vuong R, Mackie W.** The crystalline polymorphism of mannan in plant cell walls and after recrystallisation. *Planta*. 1984:161(4):320-329. https://doi.org/10.1007/BF00398722

**Chernova T, Ageeva M, Ivanov O, Lev-Yadun S, Gorshkova T.** Characterization of the fiber-like cortical cells in moss gametophytes. *Planta*. 2024:259(5):92. https://doi.org/10.1007/s00425-024-04367-5

**Chen J, Yang L, Gu J, Bai X, Ren Y, Fan T, Han Y, Jiang L, Xiao F, Liu Y, Cao S.** *MAN3* gene regulates cadmium tolerance through the glutathione-dependent pathway in *Arabidopsis thaliana*. *New Phytol.* 2015:205(2):570-582. https://doi.org/10.1111/nph.13101

**Clough SJ, Bent AF.** Floral dip: a simplified method for Agrobacterium-mediated transformation of *Arabidopsis thaliana*. *Plant J.* 1998:16(6):735-743. https://doi.org/10.1046/j.1365-313x.1998.00343.x

**Conklin PL, Norris SR, Wheeler GL, Williams EH, Smirnoff N, Last RL.** Genetic evidence for the role of GDP-mannose in plant ascorbic acid (vitamin C) biosynthesis. *Proc Natl Acad Sci USA.* 1999:96(7):4198–4203. https://doi.org/10.1073/pnas.96.7.4198

**Conklin PL, Saracco SA, Norris SR, Last RL.** Identification of ascorbic acid-deficient *Arabidopsis thaliana* mutants. *Genetics.* 2000:154(2):847–856.

https://doi.org/10.1093/genetics/154.2.847

**Dhugga KS, Barreiro R, Whitten B, Stecca K, Hazebroek J, Randhawa GS, Dolan M, Kinney AJ, Tomes D, Nichols S, Anderson P**. Guar seed beta-mannan synthase is a member of the cellulose synthase super gene family. *Science.* 2004:303(5656):363-366. https://doi.org/10.1126/science.1090908

**Dubois M, Gilles KA, Hamilton JK, Rebers PA, Smith F.** Colorimetric method for determination of sugars and related substances. *Anal Chem.* 1956:28:350-356 https://doi.org/10.1021/ac60111a017

**Goubet F, Barton CJ, Mortimer JC, Yu X, Zhang Z, Miles GP, Richens J, Liepman AH, Seffen K, Dupree P.** Cell wall glucomannan in Arabidopsis is synthesised by CSLA glycosyltransferases, and influences the progression of embryogenesis. *Plant J.* 2009:60(3):527-538. https://doi.org/10.1111/j.1365-313X.2009.03977.x

**Goubet F, Dupree P, Johansen KS.** Carbohydrate gel electrophoresis. *Methods Mol Biol*. 2011:715:81-92. https://doi.org/10.1007/978-1-61779-008-9_5

**Handford MG, Baldwin TC, Goubet F, Prime TA, Miles J, Yu X, Dupree P.** Localisation and characterisation of cell wall mannan polysaccharides in *Arabidopsis thaliana*. *Planta*. 2003:218(1):27-36. https://doi.org/10.1007/s00425-003-1073-9

**Herburger K, Głazowska S, Mravec J.** Bricks out of the wall: polysaccharide extramural functions. *Trends Plant Sci.* 2022:27(12):1231-1241. https://doi.org/10.1016/j.tplants.2022.07.008

**Hoffmann N, McFarlane HE.** Xyloglucan side chains enable polysaccharide secretion to the plant cell wall. *Dev Cell*. 2024:59(19):2609-2625.e8. https://doi.org/10.1016/j.devcel.2024.06.006

**Hogg D, Woo EJ, Bolam DN, McKie VA, Gilbert HJ, Pickersgill RW** (2001) Crystal structure of mannanase 26A from Pseudomonas cellulosa and analysis of residues involved in substrate binding. *J Biol Chem.* 2001: 276(33):31186-31192. https://doi: 10.1074/jbc.M010290200

**Iglesias-Fernández R, Rodríguez-Gacio MC, Barrero-Sicilia C, Carbonero P, Matilla A.** Three endo-β-mannanase genes expressed in the micropylar endosperm and in the radicle influence germination of *Arabidopsis thaliana* seeds. *Planta*. 2011:233(1):25-36. https://doi.org/10.1007/s00425-010-1257-z

**Jacobson T, Edwards M, Qiande M, Robert M, Moncrieff J, Voiniciuc C** (2025) Intracellular mannanases sustain matrix polysaccharide biosynthesis. *bioRxiv*. https://doi.org/10.1101/2025.02.25.640093

**Kolkas H, Burlat V, Jamet E.** Immunochemical Identification of the Main Cell Wall Polysaccharides of the Early Land Plant *Marchantia polymorpha*. *Cells*. 2023:12(14):1833. https://doi.org/10.3390/cells12141833

**Kong Y, Peña MJ, Renna L, Avci U, Pattathil S, Tuomivaara ST, Li X, Reiter WD, Brandizzi F, Hahn MG, et al.** Galactose-depleted xyloglucan is dysfunctional and leads to dwarfism in Arabidopsis. *Plant Physiol*. 2015:167(4):1296-306.

https://doi.org/10.1104/pp.114.255943

**Krogh A, Larsson B, von Heijne G, Sonnhammer EL.** Predicting transmembrane protein topology with a hidden Markov model: application to complete genomes. *J Mol Biol*. 2001:305(3):567-580. https://doi.org/10.1006/jmbi.2000.4315

**Liepman AH, Wilkerson CG, Keegstra K.** Expression of cellulose synthase-like (Csl) genes in insect cells reveals that CslA family members encode mannan synthases. *Proc Natl Acad Sci USA.* 2005:102(6):2221-2226. https://doi.org/10.1073/pnas.0409179102

**Matthysse AG, White S, Lightfoot R.** Genes required for cellulose synthesis in Agrobacterium tumefaciens. *J Bacteriol*. 1995:177(4):1069-1075. https://doi.org/10.1128/jb.177.4.1069-1075.1995

**Mayer MP, Bukau B.** Hsp70 chaperones: cellular functions and molecular mechanism. *Cell Mol Life Sci*. 2005:62(6):670-684. https://doi.org/10.1007/s00018-004-4464-6

**Mohnen D.** Pectin structure and biosynthesis. *Curr Opin Plant Biol*. 2008:11(3):266-277. https://doi.org/10.1016/j.pbi.2008.03.006

**Möller S, Croning MD, Apweiler R.** Evaluation of methods for the prediction of membrane spanning regions. *Bioinformatics*. 2001:17(7):646-53. https://doi.org/10.1093/bioinformatics/17.7.646

**Mori K.** Tripartite management of unfolded proteins in the endoplasmic reticulum. *Cell*. 2000:101(5):451-454. https://doi.org/10.1016/s0092-8674(00)80855-7

**Li KL, Nakashima K, Hisata K, Satoh N.** Expression and possible functions of a horizontally transferred glycosyl hydrolase gene, *GH6-1*, in *Ciona* embryogenesis. *Evodevo*. 2023:14(1):11. https://doi.org/10.1186/s13227-023-00215-x

**Nicol F, His I, Jauneau A, Vernhettes S, Canut H, Höfte H.** A plasma membrane-bound putative endo-1,4-beta-D-glucanase is required for normal wall assembly and cell elongation in Arabidopsis. *EMBO J.* 1998:17(19):5563-5576. https://doi.org/doi:10.1093/emboj/17.19.5563

**Nishigaki N, Yoshimi Y, Kuki H, Kunieda T, Hara-Nishimura I, Tsumuraya Y, Takahashi D, Dupree P, Kotake T.** Galactoglucomannan structure of Arabidopsis seed-coat mucilage in GDP-mannose synthesis impaired mutants. *Physiol Plant.* 2021:173(3):1244-1252. https://doi.org/10.1111/ppl.13519

**Nonogaki H, Gee OH, Bradford KJ.** A germination-specific endo-β-mannanase gene is expressed in the micropylar endosperm cap of tomato seeds. *Plant Physiol.* 2000:123(4):1235-1246. https://doi.org/10.1104/pp.123.4.1235

**Oda Y, Hosokawa N, Wada I, Nagata K.** EDEM as an acceptor of terminally misfolded glycoproteins released from calnexin. *Science*. 2003:299(5611):1394-1397. https://doi.org/10.1126/science.1079181

**Reid JS, Edwards ME, Dickson CA, Scott C, Gidley MJ.** Tobacco transgenic lines that express fenugreek galactomannan galactosyltransferase constitutively have structurally altered galactomannans in their seed endosperm cell walls. *Plant Physiol.*

644 2003:131(3):1487-1495. https://doi.org/10.1104/pp.102.016840
645 **Sawake S, Tajima N, Mortimer JC, Lao J, Ishikawa T, Yu X, Yamanashi Y, Yoshimi**
646 **Y, Kawai-Yamada M, Dupree P, et al.** KONJAC1 and 2 are key factors for GDP-
647 mannose generation and affect L-ascorbic Acid and glucomannan biosynthesis in
648 Arabidopsis. *Plant Cell.* 2015:27(12):3397-3409.
649 https://doi.org/10.1105/tpc.15.00379
650 **Schröder R, Wegrzyn TF, Bolitho KM, Redgwell RJ.** Mannan transglycosylase: a
651 novel enzyme activity in cell walls of higher plants. *Planta*. 2004:219(4):590-600.
652 https://doi.org/10.1007/s00425-004-1274-x
653 **Scheller HV, Ulvskov P.** Hemicelluloses. *Annu Rev Plant Biol.* 2010:61:263-289.
654 https://doi.org/10.1146/annurev-arplant-042809-112315
655 **Standal R, Iversen TG, Coucheron DH, Fjaervik E, Blatny JM, Valla S.** A new gene
656 required for cellulose production and a gene encoding cellulolytic activity in
657 *Acetobacter xylinum* are colocalized with the *bcs* operon. *J Bacteriol*.
658 1994:176(3):665-672. https://doi.org/10.1128/jb.176.3.665-672.1994
659 **Tamura K, Shimada T, Kondo M, Nishimura M, Hara-Nishimura I.**
660 KATAMARI1/MURUS3 Is a novel golgi membrane protein that is required for
661 endomembrane organization in Arabidopsis. *Plant Cell*. 2005:17(6):1764-76.
662 https://doi.org/10.1105/tpc.105.031930
663 **Tamura K, Stecher G, Kumar S.** MEGA11: Molecular Evolutionary Genetics Analysis
664 version 11. *Mol Biol Evol.* 2021:38(7):3022-3027.
665 https://doi.org/10.1093/molbev/msab120
666 **Teufel F, Almagro Armenteros JJ, Johansen AR, Gíslason MH, Pihl SI, Tsirigos KD,**
667 **Winther O, Brunak S, von Heijne G, et al.** SignalP 6.0 predicts all five types of
668 signal peptides using protein language models. *Nat Biotechnol.* 2022:40(7):1023-
669 1025. https://doi.org/10.1038/s41587-021-01156-3
670 **Thorne K, Urbanowicz BR, Hahn MG** (2023) Plant cell wall glycan-directed
671 monoclonal antibodies. In: Plant cell walls - Research Milestones and Conceptual
672 Insights (Ed., Geitmann, A.). Boca Raton: CRC Press, Taylor & Francis Group, pp.
673 206-236. https://doi.org/10.1201/9781003178309
674 **Verbančič J, Lunn JE, Stitt M, Persson S.** Carbon supply and the regulation of cell wall
675 synthesis. *Mol Plant.* 2018:11(1):75-94. https://doi.org/10.1016/j.molp.2017.10.004
676 **Voiniciuc C.** Modern mannan: a hemicellulose's journey. *New Phytol.* 2022:234(4):1175-
677 1184. https://doi.org/10.1111/nph.18091
678 **Voiniciuc C, Schmidt MH, Berger A, Yang B, Ebert B, Scheller HV, North HM,**
679 **Usadel B, Günl M.** MUCILAGE-RELATED10 produces galactoglucomannan that
680 maintains pectin and cellulose architecture in Arabidopsis seed mucilage. *Plant*
681 *Physiol.* 2015:169(1):403-420. https://doi.org/10.1104/pp.15.00851
682 **Wang Y, Azhar S, Gandini R, Divne C, Ezcurra I, Aspeborg H.** Biochemical
683 characterization of the novel endo-beta-mannanase AtMan5-2 from *Arabidopsis*

*thaliana*. *Plant Sci.* 2015:**241**:151-63. https://doi.org/10.1016/j.plantsci.2015.10.002

**Wang Y, Mortimer JC, Davis J, Dupree P, Keegstra K.** Identification of an additional protein involved in mannan biosynthesis. *Plant J.* 2013:73(1):105-117. https://doi.org/10.1111/tpj.12019

**Wang Y, Vilaplana F, Brumer H, Aspeborg H.** Enzymatic characterization of a glycoside hydrolase family 5 subfamily 7 (GH5_7) mannanase from *Arabidopsis thaliana*. *Planta.* 2014:239(3):653-665. https://doi.org/10.1007/s00425-013-2005-y

**Winter D, Vinegar B, Nahal H, Ammar R, Wilson GV, Provart NJ.** An "Electronic Fluorescent Pictograph" browser for exploring and analyzing large-scale biological data sets. PLoS One. 2007:2(8):e718. https://doi.org/10.1371/journal.pone.0000718

**Wu Q, Meng YT, Feng ZH, Shen RF, Zhu XF.** The endo-beta mannase MAN7 contributes to cadmium tolerance by modulating root cell wall binding capacity in *Arabidopsis thaliana*. *J Integr Plant Biol.* 2023:65(7):1670-1686. https://doi.org/10.1111/jipb.13487

**Yoshimi Y, Yu L, Cresswell R, Guo X, Echevarría-Poza A, Lyczakowski JJ, Dupree R, Kotake T, Dupree P.** Glucomannan engineering highlights the role of galactosyl modification in fine-tuning cellulose-glucomannan interaction in Arabidopsis cell walls. *Nat Commun*. 2025:16(1):1235. https://doi.org/10.1038/s41467-025-56626-y

**Yu L, Lyczakowski JJ, Pereira CS, Kotake T, Yu X, Li A, Mogelsvang S, Skaf MS, Dupree P.** The patterned structure of galactoglucomannan suggests it may bind to cellulose in seed mucilage. *Plant Physiol.* 2018:178(3):1011-1026. https://doi.org/10.1104/pp.18.00709

**Yu L, Yoshimi Y, Cresswell R, Wightman R, Lyczakowski JJ, Wilson LFL, Ishida K, Stott K, Yu X, Charalambous S, Wurman-Rodrich J, Terrett OM, Brown SP, Dupree R, Temple H, Krogh KBRM, Dupree P.** Eudicot primary cell wall glucomannan is related in synthesis, structure, and function to xyloglucan. *Plant Cell*. 2022:34(11):4600-4622. https://doi.org/10.1093/plcell/koac238

**Yu L, Shi D, Li J, Kong Y, Yu Y, Chai G, Hu R, Wang J, Hahn MG, Zhou G.** CELLULOSE SYNTHASE-LIKE A2, a glucomannan synthase, is involved in maintaining adherent mucilage structure in Arabidopsis seed. *Plant Physiol.* 2014:164(4):1842-1856. https://doi.org/10.1104/pp.114.236596

**Zhang R, Li B, Zhao Y, Zhu Y, Li L.** An essential role for mannan degradation in both cell growth and secondary cell wall formation. *J Exp Bot.* 2023:75(5):1407-1420. https://doi.org/10.1093/jxb/erad463

**Zhao Y, Song D, Sun J, Li L.** *Populus* endo-beta-mannanase PtrMAN6 plays a role in coordinating cell wall remodeling with suppression of secondary wall thickening through generation of oligosaccharide signals. *Plant J.* 2013:74(3):473-85. https://doi.org/10.1111/tpj.12137

**Zhou Y, Jiang R, Perkins WS, Cheng Y.** Morphology evolution and gelation mechanism of alkali induced konjac glucomannan hydrogel. *Food Chem.* 2018:269:80-88.

https://doi.org/10.1016/j.foodchem.2018.05.116

**Zhong R, Cui D, Ye ZH.** Members of the DUF231 family are *O*-acetyltransferases catalyzing 2-*O*- and 3-*O*-acetylation of mannan. *Plant Cell Physiol.* 2018:59(11):2339-2349. https://doi.org/10.1093/pcp/pcy159

729 **FIGURE LEGENDS**

730 **Figure 1. Distribution of TM-type MANs in plants.**

731 (A) Schematic models of AtMAN proteins. The signal peptide and TM region were
732 identified with the aid of SignalP 6.0 and TMHMM 2.0 programs, respectively. (B)
733 Phylogenetic tree of plant MANs. Phylogenetic relationships of MANs from Arabidopsis
734 and other plants including *S. moellendorffii*, *P. patens*, and *M. polymorpha* were analyzed
735 with MEGA software (version 11.0). Rice OsMAN5 and poplar PtrMAN6 indicated with
736 pink dots have HHEL and HDDL sequences at the C-terminus instead of HDEL,
737 respectively. SmMAN2 with the orange dot has a TM domain in the N-terminal region
738 that its neighbor, SmMAN3, lacks. MAN sequences from angiosperms are shown in black
739 whereas those from other organisms are in blue. Amt, amborella; Lj, *Lotus japonicus*; Mp,
740 *M. polymorpha*; Os, rice; Pp, *P. patens*; Sm, *S. moellendorffii*. AnMAN5A from
741 *Aspergillus nidulans* was used as the outgroup. Numbers in the nodes represent bootstrap
742 values. The accession numbers and abbreviated names for these sequences are listed in
743 Supplementary Table S2.

744

745 **Figure 2. Reduced glucomannan accumulation in the cell walls of *man* mutants.**

746 Cross sections from the bottom part of the first inflorescence stem of *man* mutants were
747 compared with WT and the *csla2-2 csla9-2* double mutant. The images for dark field and
748 glucomannan signals with LM21 antibody are shown. The bars indicate 100 μm.

749

750 **Figure 3. Cell wall fractions and mannose content in *man* mutants.**

751 (A) Relative sugar content of cell wall fractions in the *man* mutants. Sugar content of
752 soluble, alkali, and cellulose fractions from the bottom part of inflorescence stems was
753 quantified by the phenol-sulfuric acid method (Supplementary Fig. S4). (B) Mannose
754 content of cell wall fractions. The content was calculated based on the sugar content and
755 the monosaccharide composition of cell wall fractions (Supplementary Fig. S5). The
756 values are shown in weight per gram fresh weight (g fw). Data are mean values with
757 standard deviation (three biological replicates). Different letters indicate significant
758 differences determined with the Tukey HSD test ($p < 0.05$).
759
760 **Figure 4. Change in β-GGM and AcGGM.**
761 GGMs included in the cell walls of the bottom part of inflorescence stems were
762 hydrolyzed into specific oligosaccharides such as MGM, GBGM, $(GA)_2GM$
763 (Supplementary Fig. S6), which were labelled with a fluorescent compound then
764 separated in the gel. Here, *man* mutants were compared with WT, *csla2-1 csla9-1* double
765 mutants known to lack stem glucomannans, and the *msr1-1 msr2-1* double mutant with
766 reduced glucomannan (Goubet et al. 2009; Wang et al. 2013). The sugar symbols follow
767 the international glycan code nomenclature (www.ncbi.nlm.nih.gov/glycans/snfg.html).
768 The oligosaccharide structures are shown on the right. The results for control reactions
769 are shown in Supplementary Fig. S7.
770
771 **Figure 5. Glucomannan particles inside cells.**
772 (*A*) Magnified images of xylem and interfascicular fiber cells. The merged image of

773 calcofluor staining and glucomannan signals with LM21 antibody are shown. The bars
774 indicate 50 μm. Arrowheads indicate relatively large (>1 μm) glucomannan signals found
775 inside cells. (*B*) Numbers of glucomannan particles in the pith, xylem, and interfascicular
776 fiber cells. The values shown are the number of particles per cell. Data are mean values
777 with standard deviation (WT, n = 6; *man6-1*, n = 6; *man2-1 man5-1*, n = 6; *man2-1 man5-*
778 *1 man6-1*, n = 6; *csla2-2 csla9-2*, n = 5). The asterisk indicates significant difference from
779 WT (Student's t test, *, $P < 0.05$). (C) Observation by immunoelectron microscopy.
780 Ultrathin sections prepared from the bottom part of the inflorescence stem of WT, *man6-*
781 *1* single, *man2-1 man5-1* double, and *man2-1 man5-1 man6-1* triple mutants were
782 observed. Glucomannan was detected with LM21 antibody. The gold particles found in
783 the cell walls are shown as red dots and those in the cytoplasm including the vacuole are
784 shown as blue dots. Representative images are shown. CP, chloroplast; CW, cell wall; V,
785 vacuole. The bars indicate 1 μm.
786
787 **Figure 6. Subcellular localization of MAN-mNeon proteins.**
788 Xylem and interfascicular fiber cells expressing AtMAN2TM-mNeon (A-E) and
789 AtMAN5TM-mNeon (F-J), and vessels expressing AtMAN6signal-mNeon (K-O) in the
790 top part of the inflorescence stem were observed with a confocal microscope. Images for
791 mNeonGreen (A, F, K), autofluorescence (B, G, L), FM 4-64FX staining (C, H, M), and
792 transmitted photomultiplier tube (D, I, N) were obtained and merged (E, J, O). The bars
793 indicate 5 μm. Schematic diagrams for each mNeonGreen (mNeon)-MAN protein are
794 shown above the merged images (E, J, O). The representative mNeonGreen signals in the

795 endomembrane system including the Golgi apparatus are indicated by yellow arrowheads
796 and those in vessels with by arrowheads. The gene constructs and the complementation
797 of the triple mutants with *pMAN2:MAN2TM-mNeon* and *pMAN5:MAN5TM-mNeon* are
798 shown in Supplementary Fig. S9. Images of the tissue localization of these MAN-mNeon
799 proteins and longitudinal sections for AtMAN6signal-mNeon are shown in
800 Supplementary Fig. S10.
801

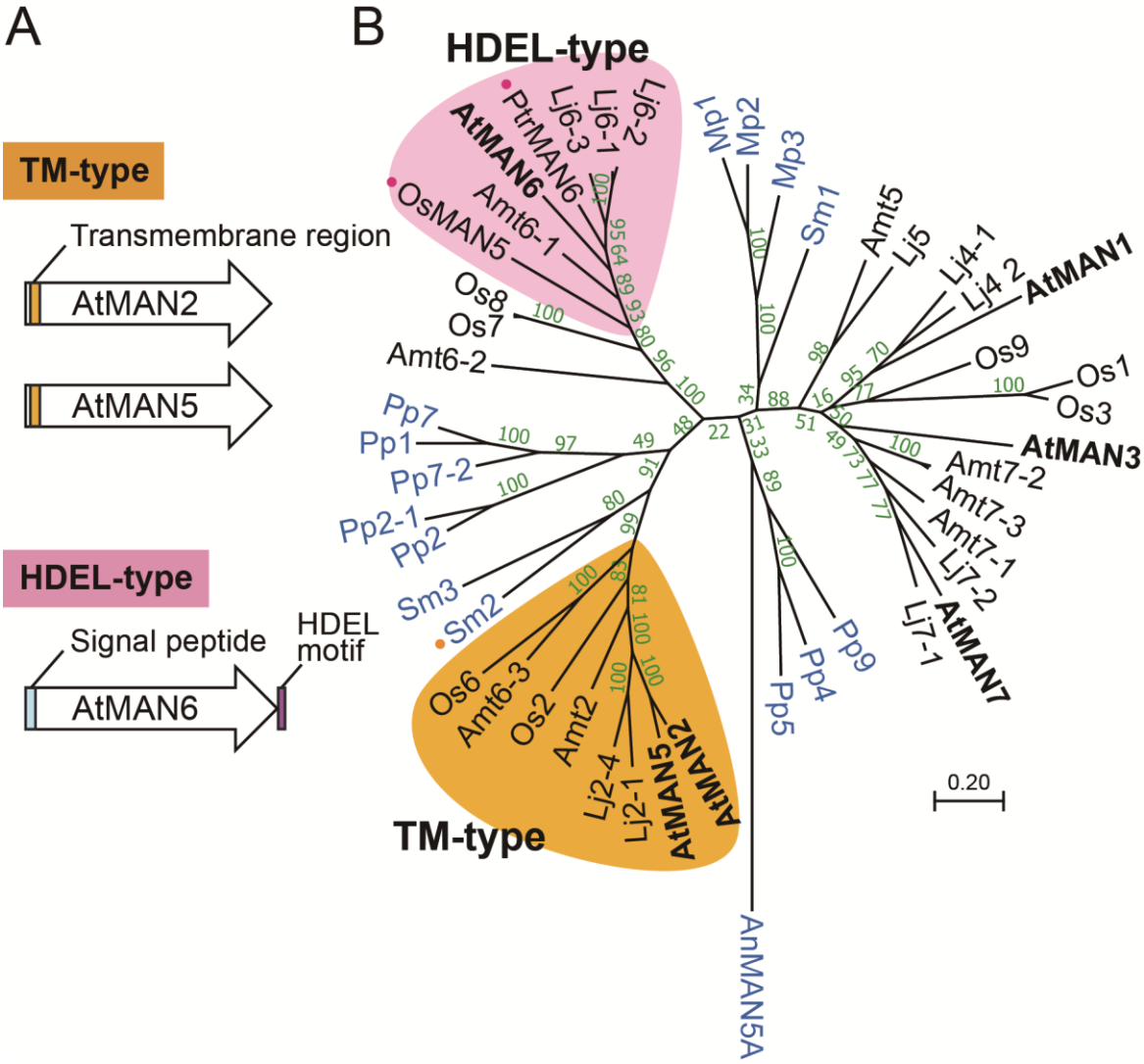
A
TM-type
Transmembrane region
AtMAN2
AtMAN5
HDEL-type
Signal peptide
HDEL motif
AtMAN6
B
HDEL-type
TM-type
Lj6-2
Lj6-1
Lj6-3
PtrMAN6
AtMAN6
OsMAN5
Amt6-1
Os8
Os7
Amt6-2
Pp7
Pp1
Pp7-2
Pp2-1
Pp2
Sm3
Sm2
Os6
Amt6-3
Os2
Amt2
Lj2-4
Lj2-1
AtMAN5
AtMAN2
Mp1
Mp2
Mp3
Sm1
Amt5
Lj5
Lj4-1
Lj4 2
AtMAN1
Os9
Os1
Os3
AtMAN3
Amt7-2
Amt7-3
Amt7-1
Lj7-2
Lj7-1
AtMAN7
Pp9
Pp4
Pp5
AnMAN5A
0.20

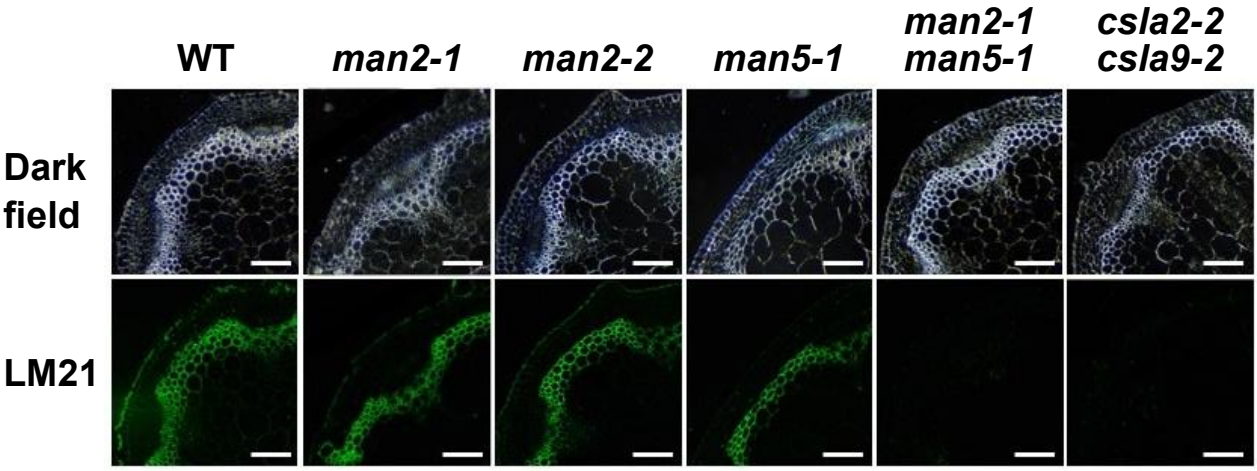
WT
man2-1
man2-2
man5-1
man2-1
man5-1
csla2-2
csla9-2
Dark field
LM21

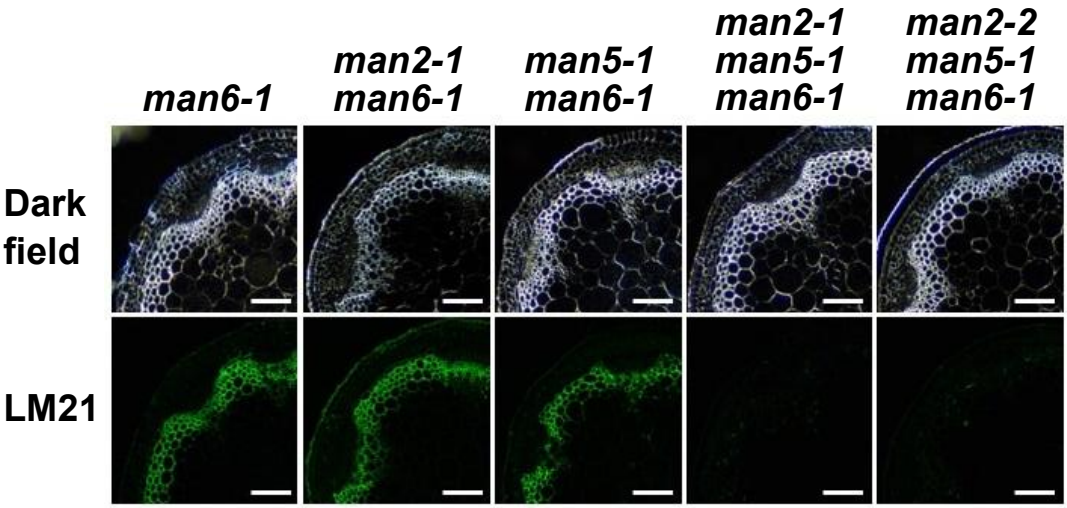
man6-1
man2-1
man6-1
man5-1
man6-1
man2-1
man5-1
man6-1
man2-2
man5-1
man6-1
Dark field
LM21

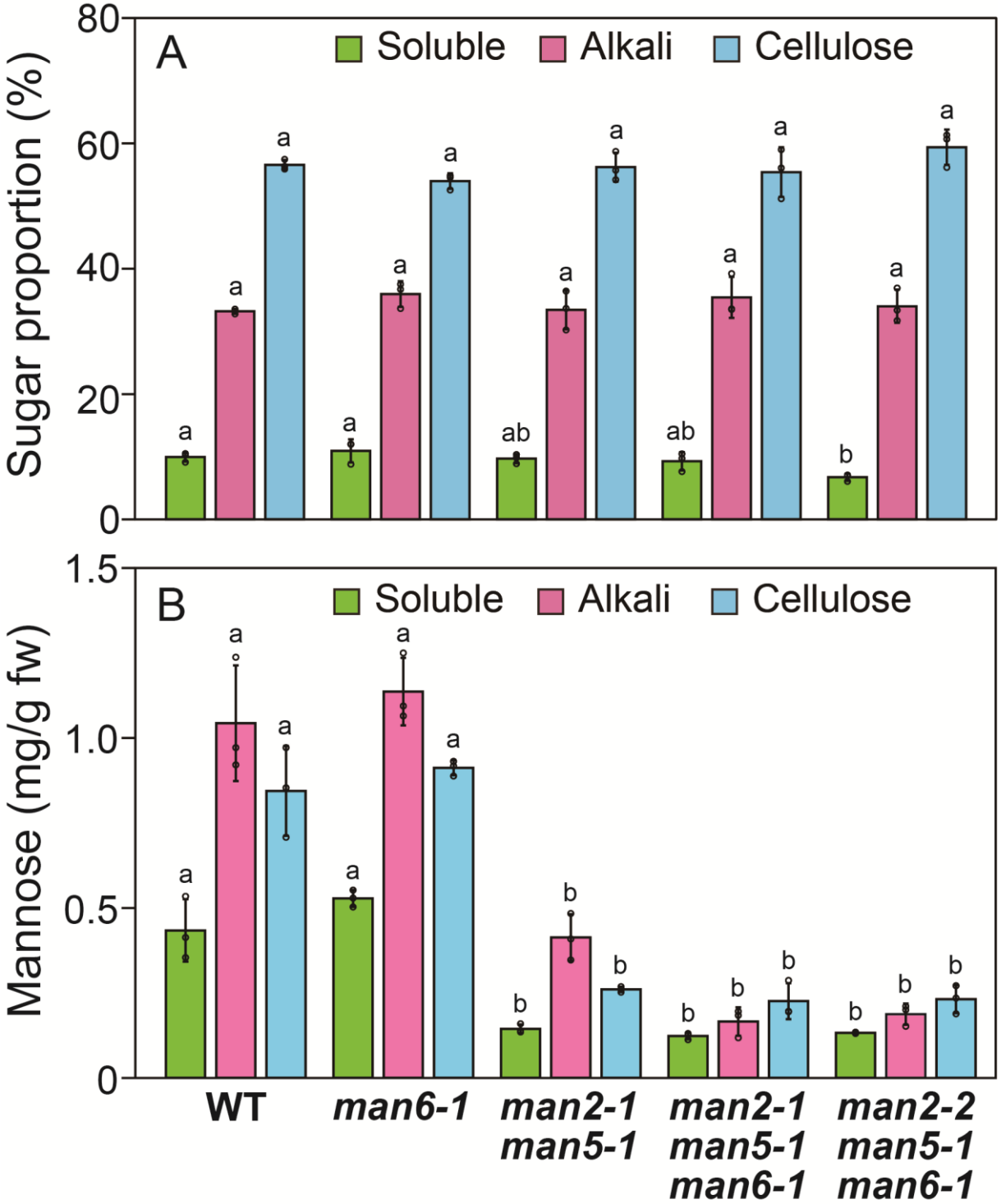
A
Soluble
Alkali
Cellulose
Sugar proportion (%)
80
60
40
20
0
a
a
a
a
a
a
ab
a
a
ab
a
a
b
a
a
B
Soluble
Alkali
Cellulose
Mannose (mg/g fw)
1.5
1.0
0.5
0
a
a
a
a
a
a
b
b
b
b
b
b
b
b
b
WT
man6-1
man2-1 man5-1
man2-1 man5-1 man6-1
man2-2 man5-1 man6-1

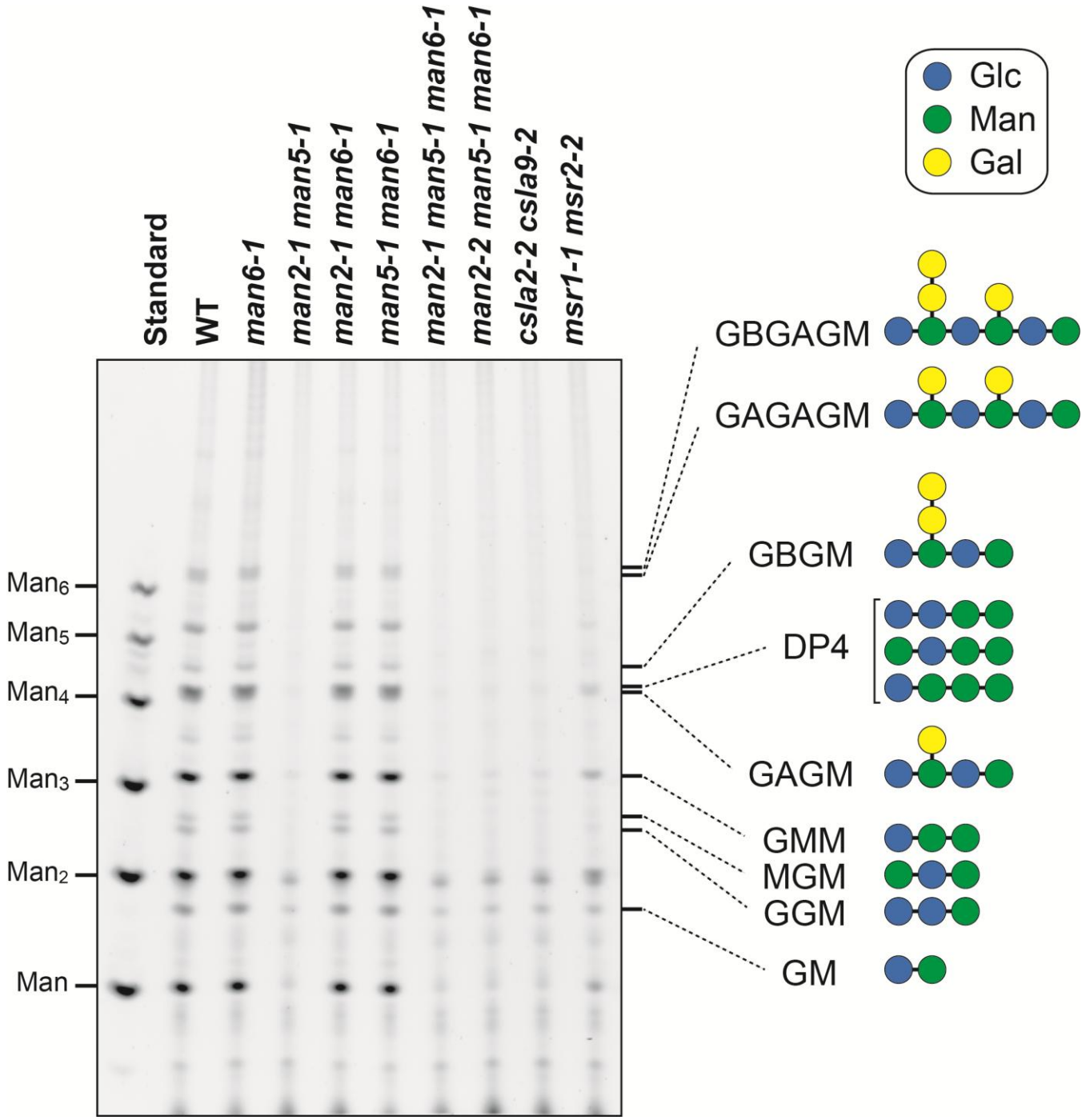
Standard
WT
man6-1
man2-1 man5-1
man2-1 man6-1
man5-1 man6-1
man2-1 man5-1 man6-1
man2-2 man5-1 man6-1
csla2-2 csla9-2
msr1-1 msr2-2
Man6
Man5
Man4
Man3
Man2
Man
Glc
Man
Gal
GBGAGM
GAGAGM
GBGM
DP4
GAGM
GMM
MGM
GGM
GM

A

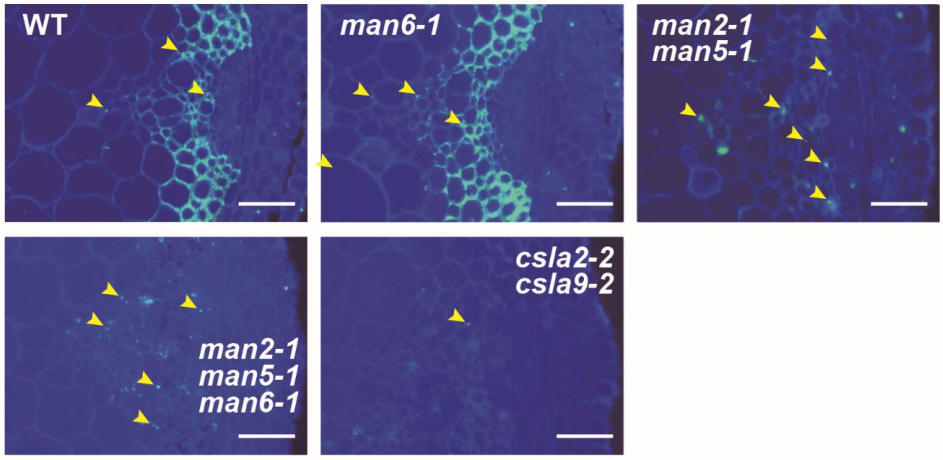
WT
man6-1
man2-1
man5-1
man2-1
man5-1
man6-1
csla2-2
csla9-2

B

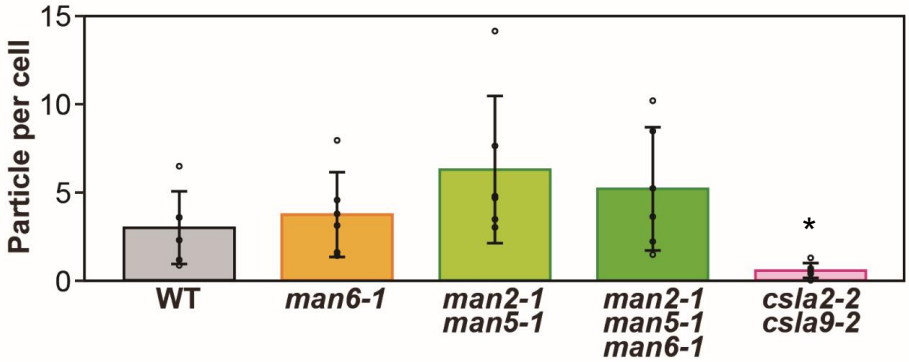
Particle per cell
15
10
5
0
*
WT
man6-1
man2-1
man5-1
man2-1
man5-1
man6-1
csla2-2
csla9-2

C

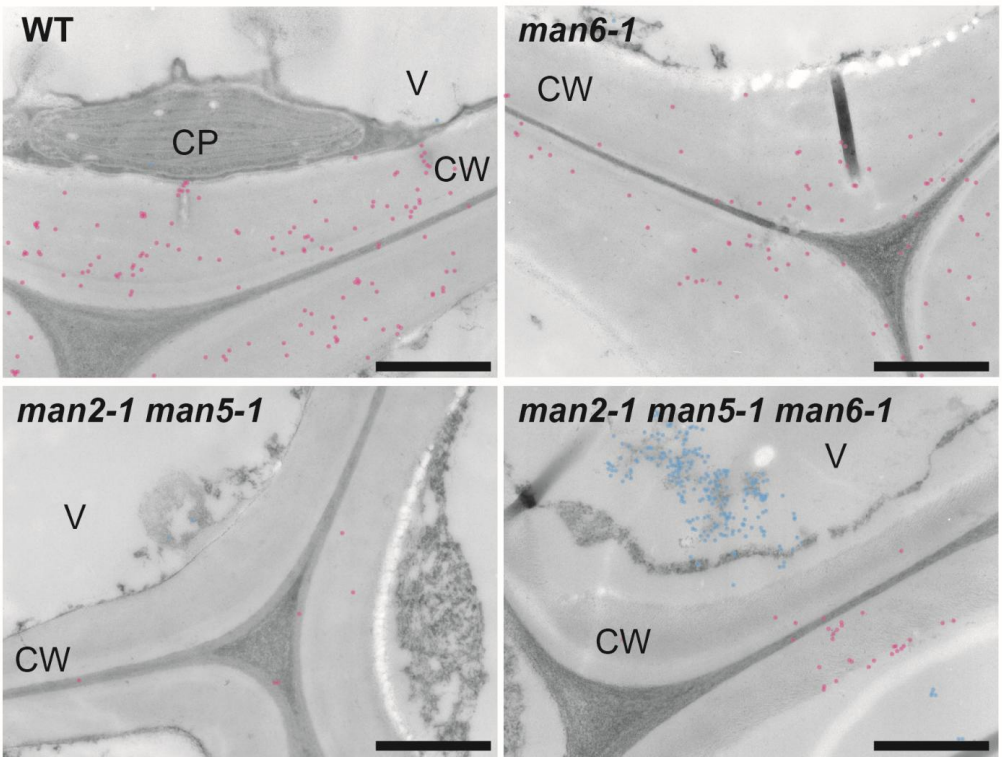
WT
V
CP
CW
man6-1
CW
man2-1 man5-1
V
CW
man2-1 man5-1 man6-1
V
CW

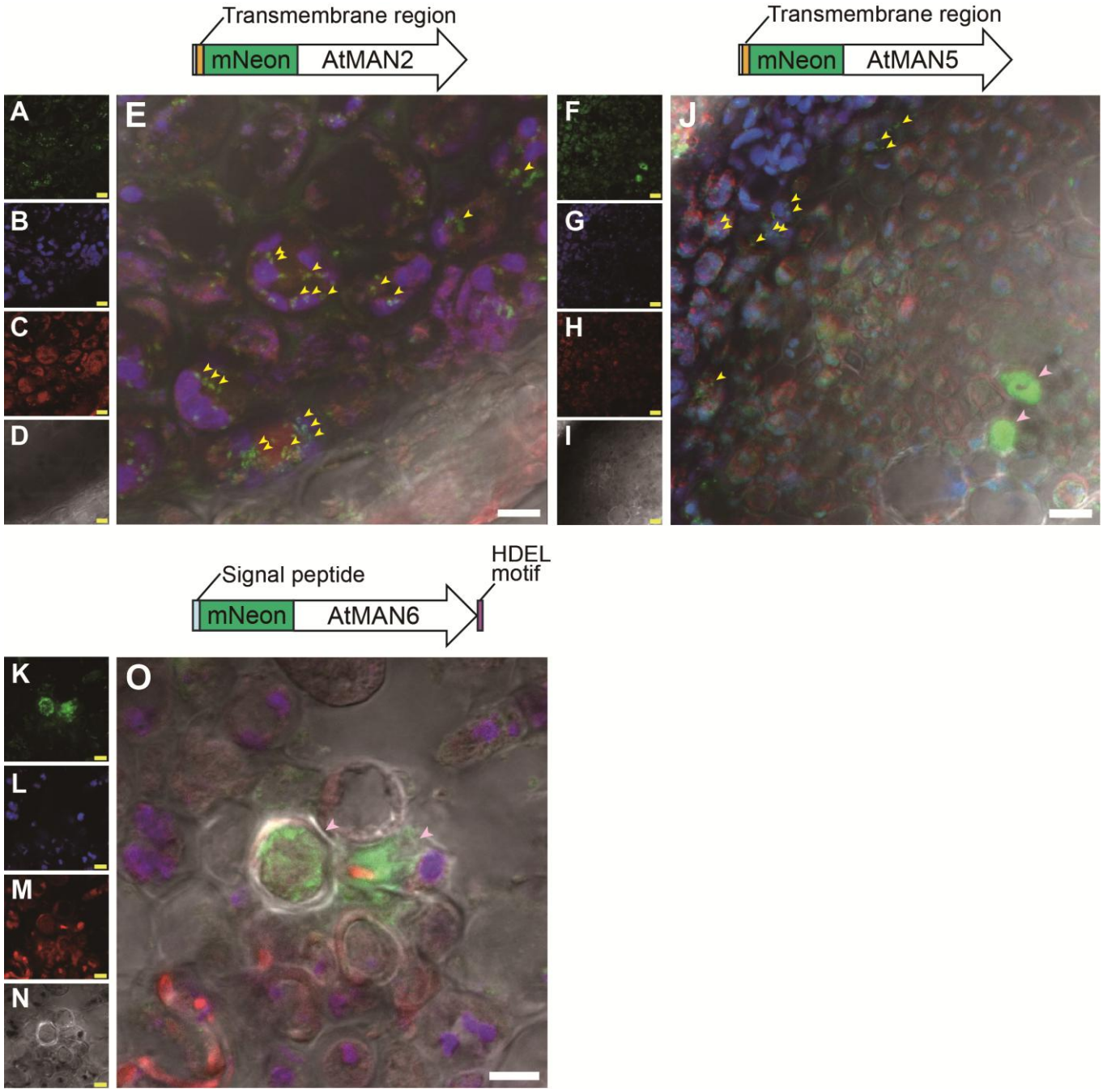
Transmembrane region
mNeon
AtMAN2
Transmembrane region
mNeon
AtMAN5
A
B
C
D
E
F
G
H
I
J
Signal peptide
HDEL motif
mNeon
AtMAN6
K
L
M
N
O